Impact of changes to the radiation transfer parametrisations plus cloud optical properties in the ECMWF model

J.-J. Morcrette, Mon.Wea.Rev., 118, 847-873

Discussion

Comparison of “old” vs. “new” RT schemes

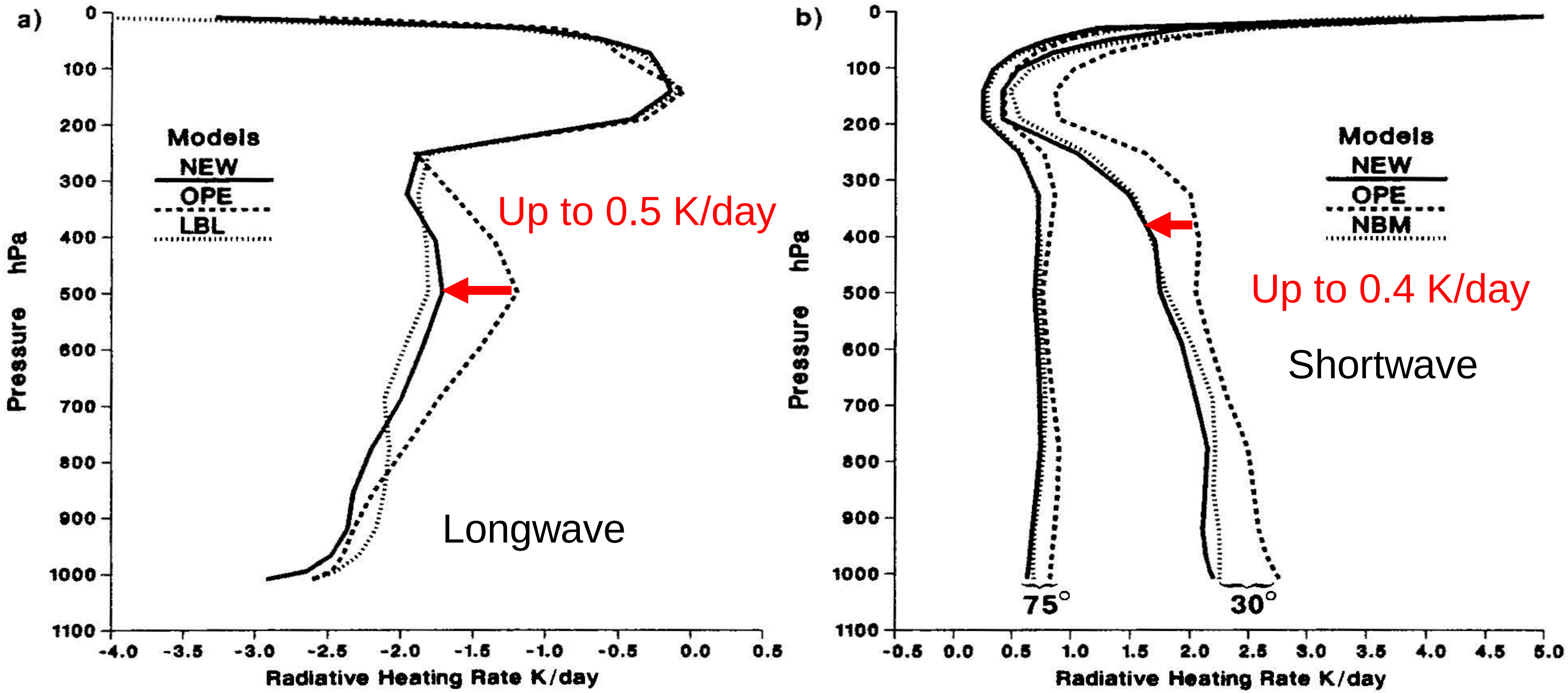

FIG. 1. Comparison of longwave radiative heating rate profiles in a clear-sky standard midlatitude summer atmosphere. OPE and NEW refer to the operational and new radiation schemes. In the longwave range (Fig. 1a), LBL (dotted line) refers to the results of the GFDL line-by-line model. In the shortwave range (Fig. 1b), NBM (dotted line) refers to the results of the narrow-band model of Fouquart et al. (1990). Shortwave results are presented for a surface albedo $A_s = 0.2$ and for two solar zenith angles, 30° and 75°.

Better agreement with reference calculations in both LW and SW. In LW, increased cooling, in SW, reduced heating, -> more net clear-sky radiative cooling.

Impact on globally averaged quantities

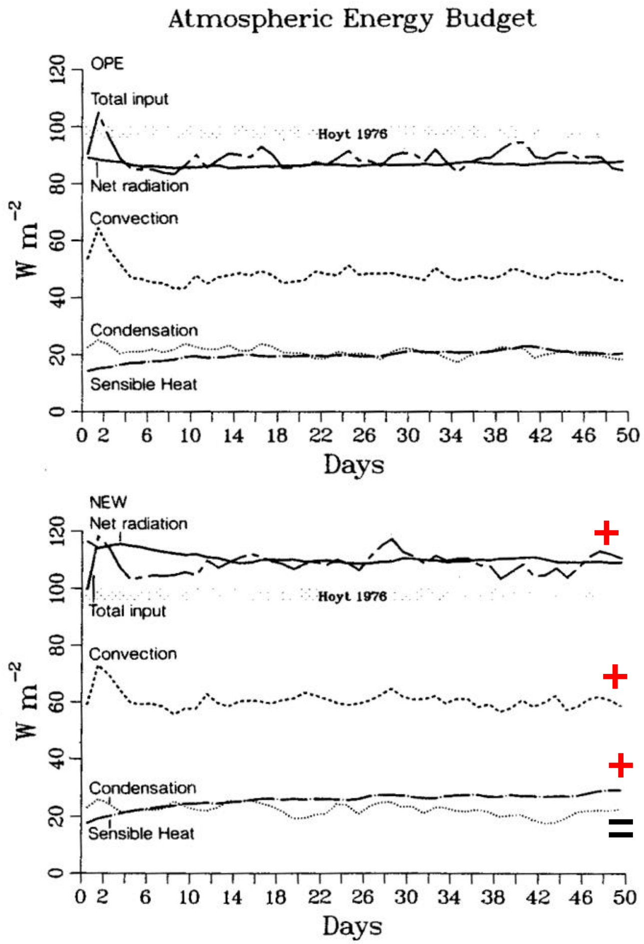

FIG. 2. Time evolution of diabatic heating due to radiation, cumulus convection, large-scale condensation, and turbulent heat transfer for the whole globe in operational forecast (top) and forecast with new radiation scheme (bottom). Initial date is 1 June 1987 (12Z). Results are for the first 50 days of T42 90-day integrations. Climatological radiation data from van Hoyt (1976).

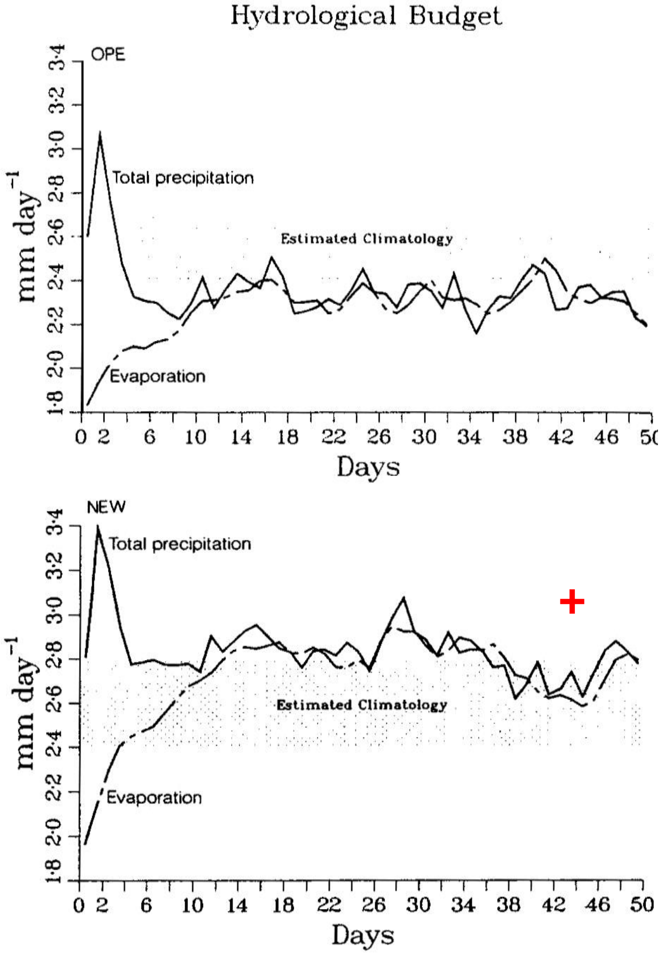

FIG. 3. As in Fig. 2, but for total precipitation and surface evaporation. Climatological precipitation data are from Jaeger (1976).

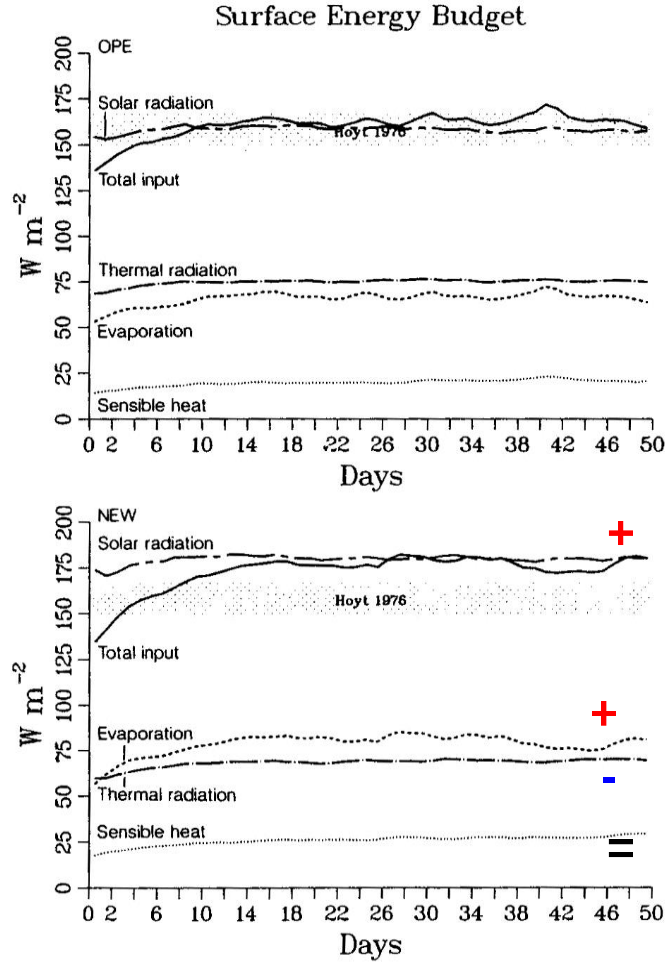

FIG. 4. As in Fig. 2, but for the components of the surface energy budget, namely net solar radiation, net thermal radiation, sensible and latent heat fluxes. Climatological radiation data from van Hoyt (1976).

T42 90-day simulations for JJA

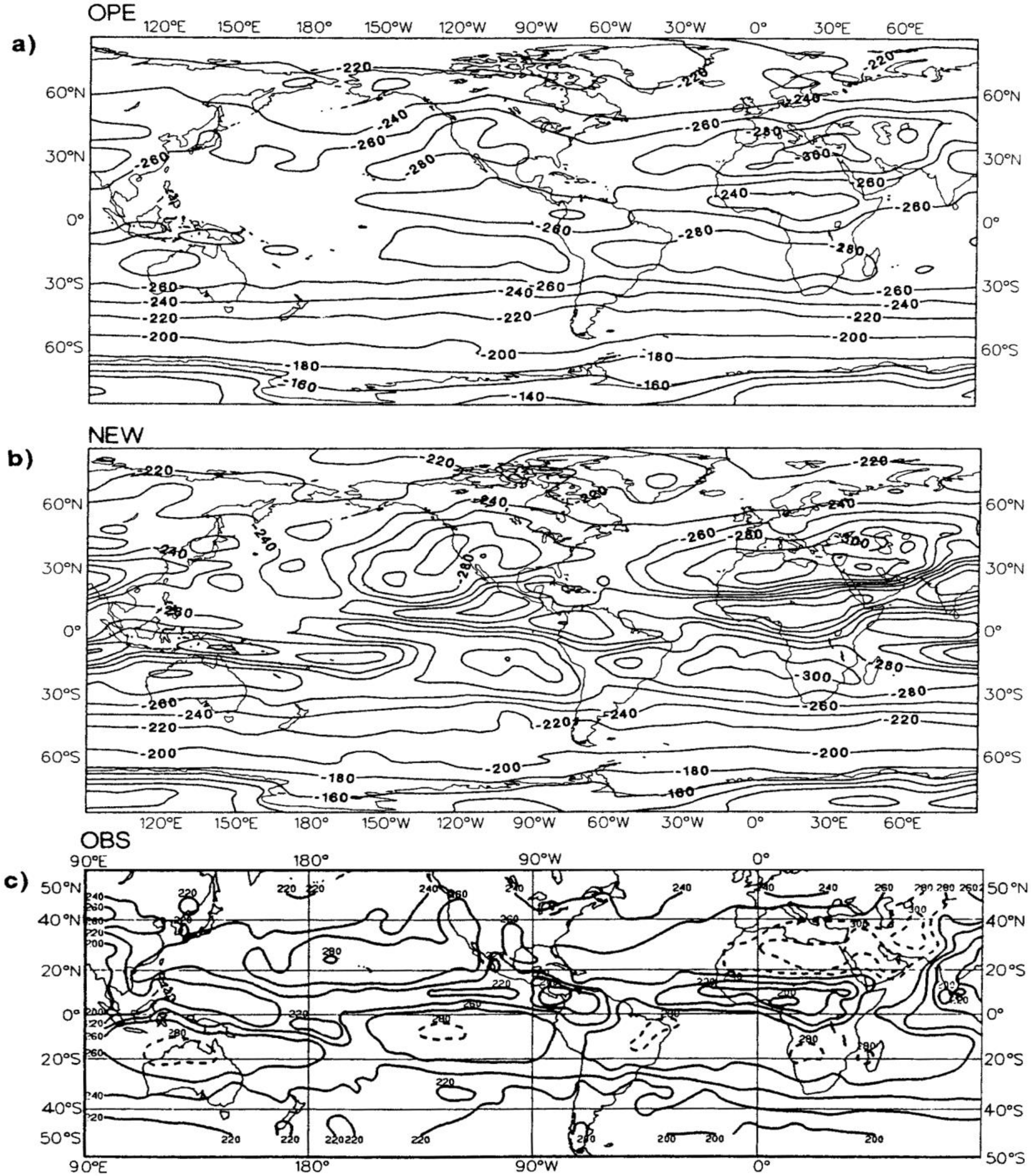

FIG. 5. Outgoing longwave radiation at the top of the atmosphere averaged over the last 30 days of T42 90-day integrations with OPE (top) and NEW (middle). Initial date is 1 June 1987 (12Z). Bottom figure is the 30-day mean OLR operationally derived by NOAA from AVHRR measurements (NOAA 1988). Interval is 20 W m^{-2}. In bottom figure, dash lines for values above 280 W m^{-2}.

Old scheme

New scheme

Cloud LW radiative effect is more marked. Increased contrast between clear- and cloudy-sky areas

Derived from NOAA-AVHRR radiances

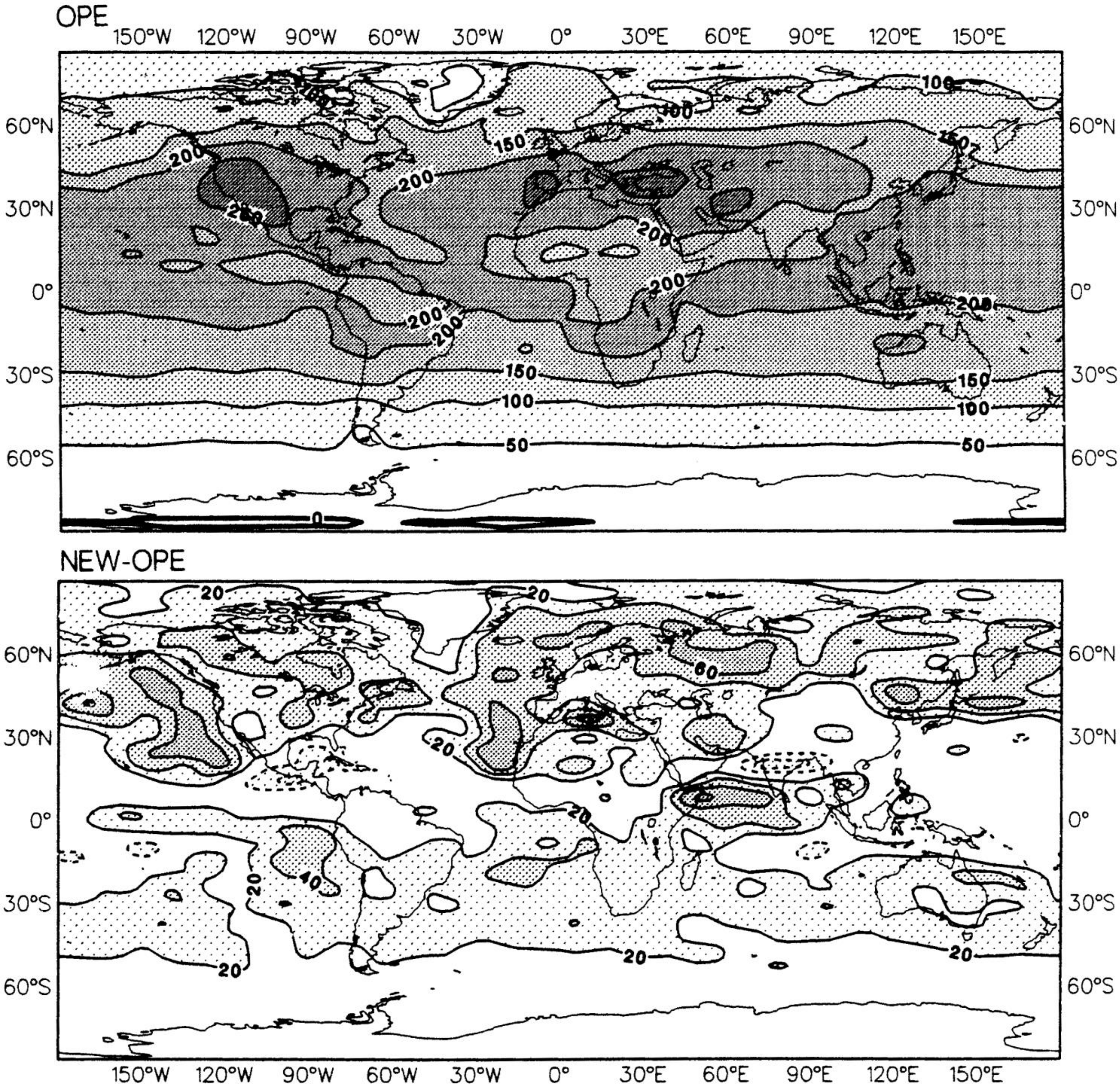

FIG. 7. As in Fig. 6, but for net solar radiation at the surface. Intervals are 50 and 20 W m^{-2}, respectively.

Increase in downward SW radiation over most of the globe linked to decrease in SW H_2O absorption

ECMWF

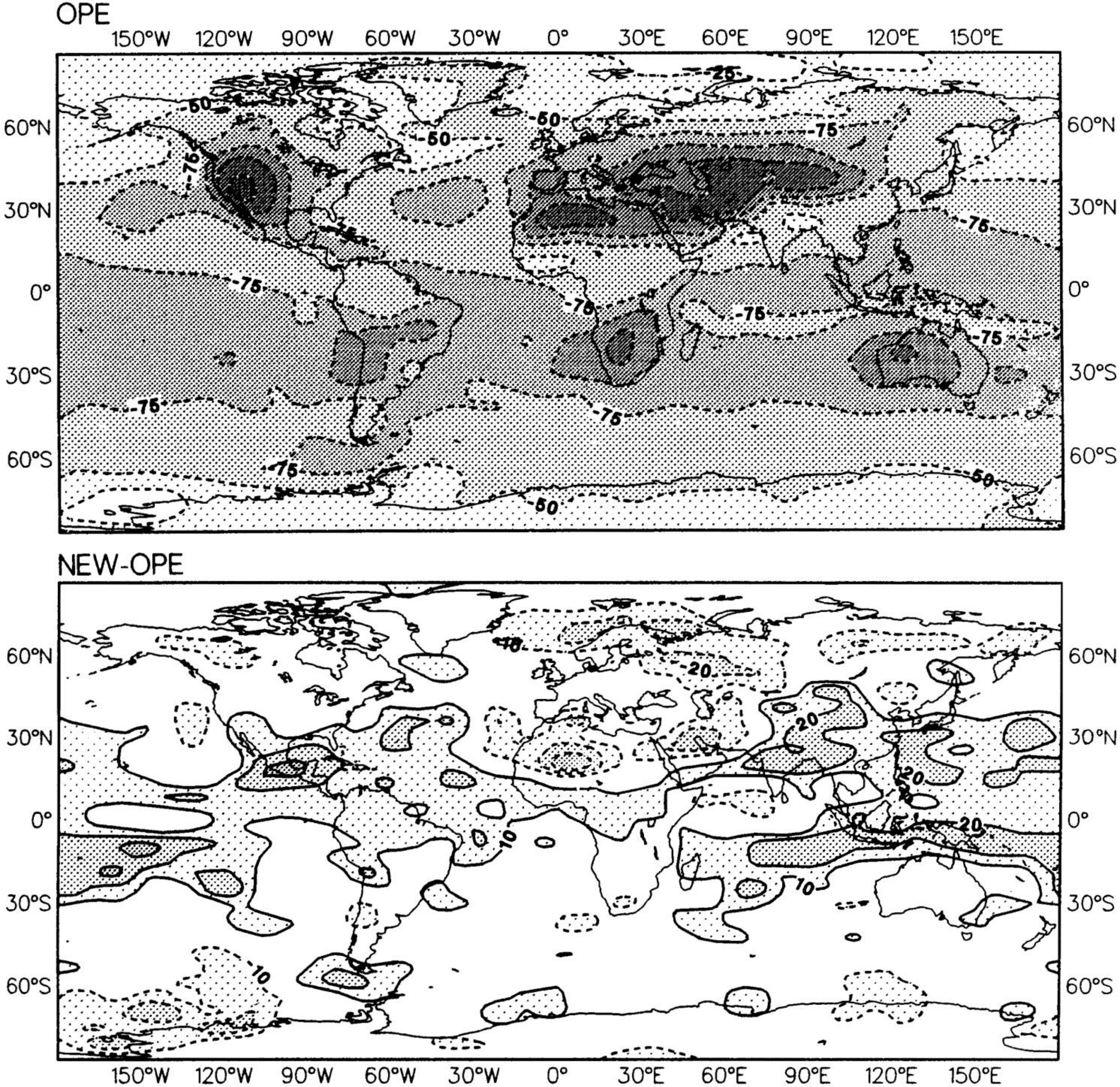

FIG. 8. As in Fig. 6, but for net longwave radiation at the surface. Intervals are 25 and 10 W m^{-2}, respectively.

Decrease in net surface LW in the tropics = larger downward radiation linked to changes in the continuum and in T and P dependence of the LW absorption in the new scheme

ECMWF

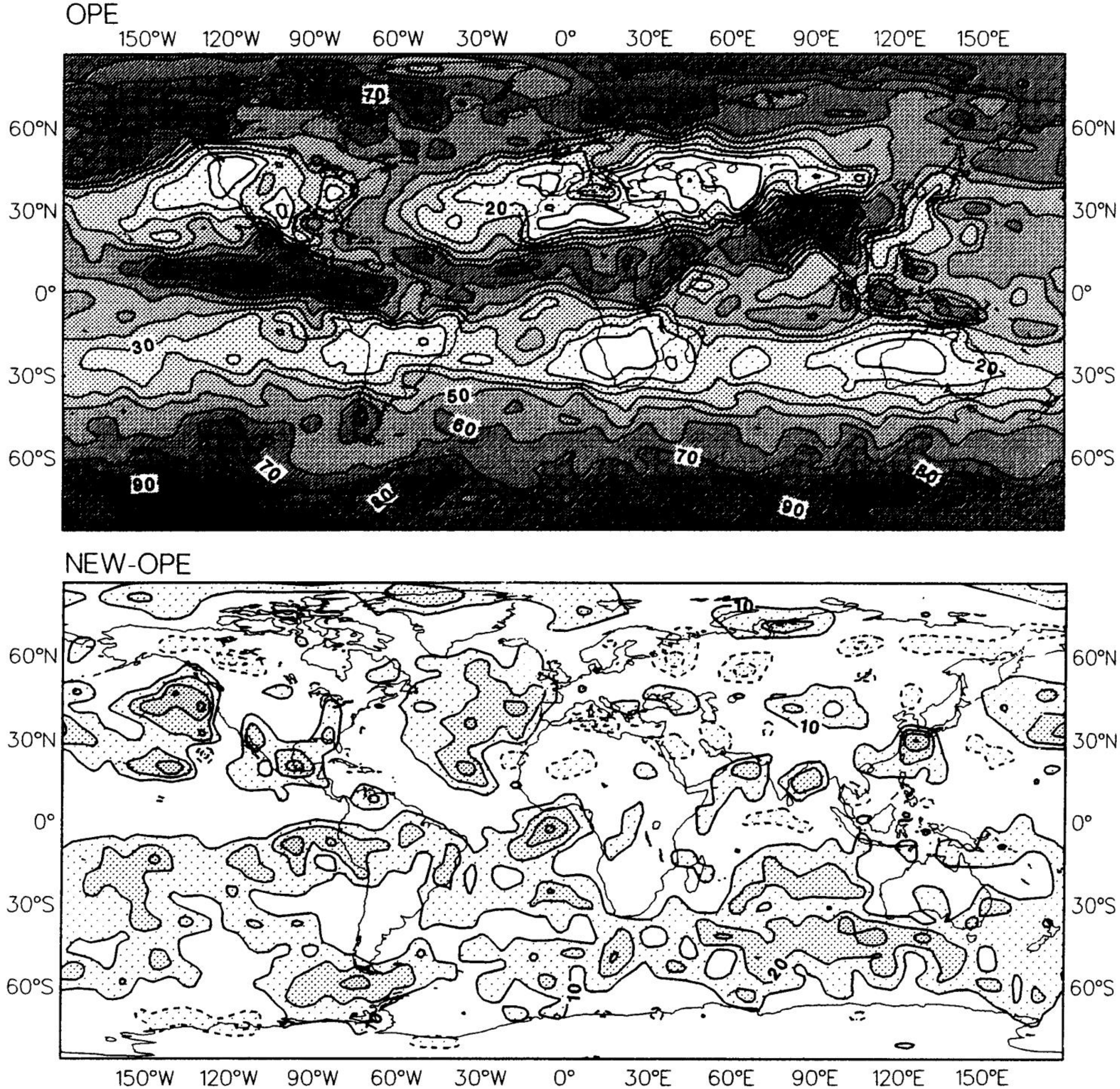

FIG. 9. As in Fig. 6, but for total cloudiness. Intervals are 10 percent on both figures.

Mostly increase in total cloudiness, most of it occurring as high clouds

ECMWF

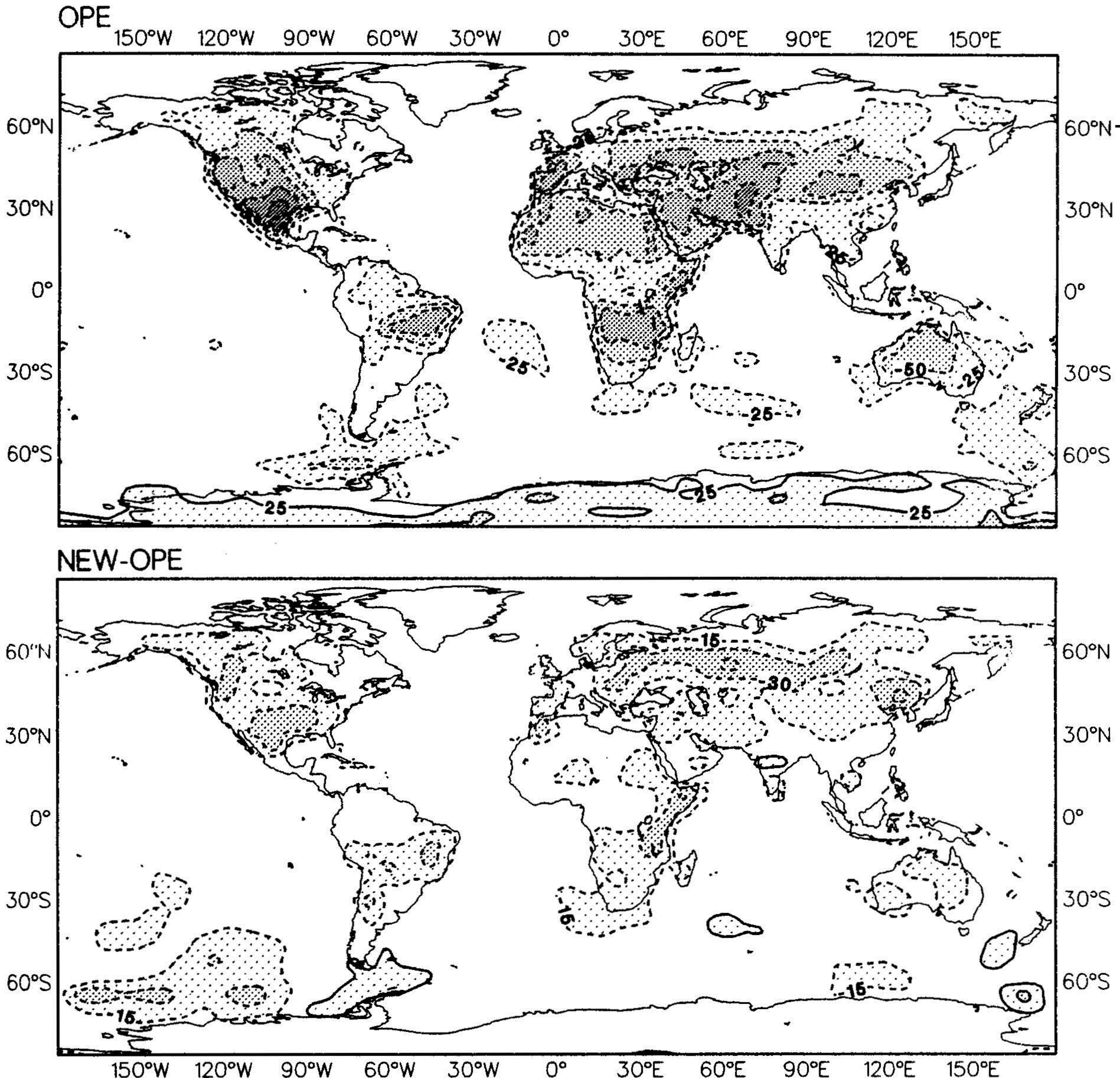

FIG. 10. As in Fig. 6, but for sensible heat flux. Intervals are 25 and 15 W m^{-2}, respectively.

Increase in the sensible heat flux coming out of the continents, linked to increased downward radiation (SW+LW)

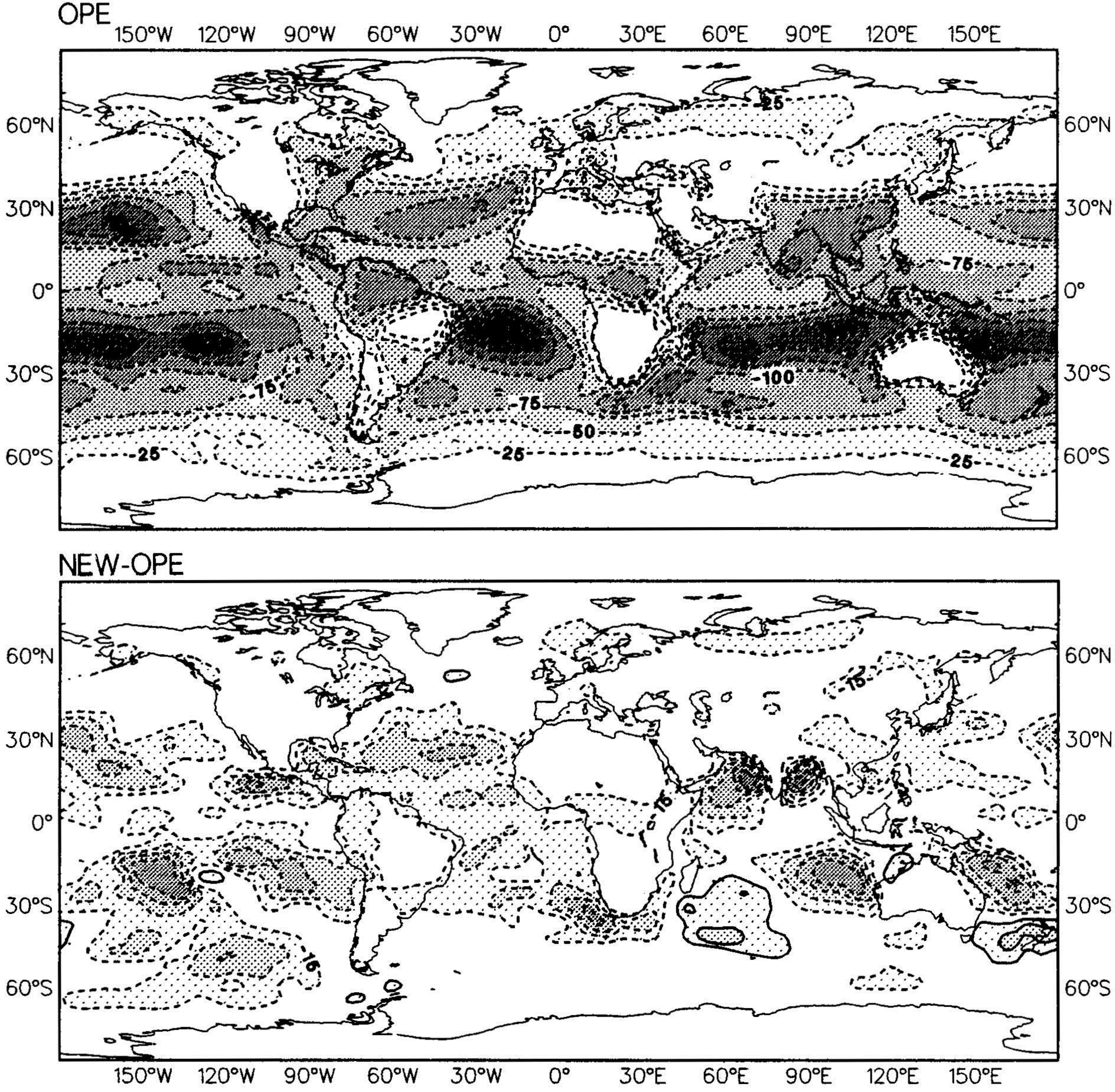

FIG. 11. As in Fig. 6, but for latent heat flux. Intervals are 25 and 15 W m^{-2}, respectively.

Increase in the latent heat flux over the oceans. Both SH and LH increases are linked to increase in available SW (+LW) radiation at the surface.

The model is run with specified SST and specified surface albedo. Increase in downward SW will not affect SST, but a slightly cooler atmosphere above the surface will enhance both SH and LH.

ECMWF

Impact on radiative and convective heating

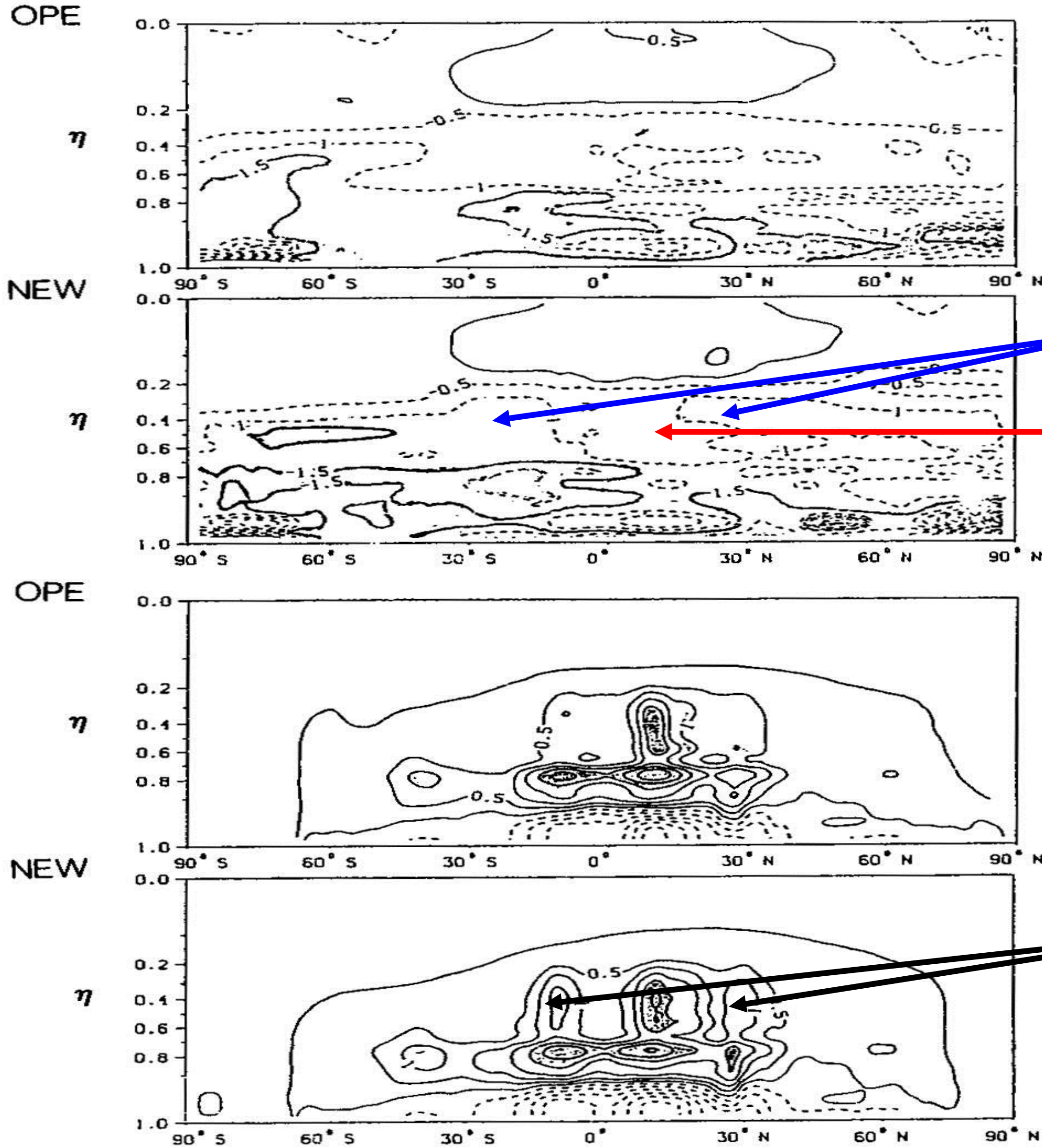

Decrease in net radiative heating

Increase in net radiative heating

Clouds are more efficient at trapping outgoing LW radiation

Increased convective activity

FIG. 12. Contribution of radiation and cumulus convection to the total diabatic heating. From top to bottom, OPE radiative heating, NEW radiative heating, OPE heating by cumulus convection, and NEW heating by cumulus convection. All quantities are in K day^{-1}, and correspond to a 30-day average between days 61 and 90 of integrations starting 1 June 1987 (12Z). Interval is 0.5 K day^{-1}; positive quantities between full lines, negative quantities between dashed lines.

Impact on total precipitation

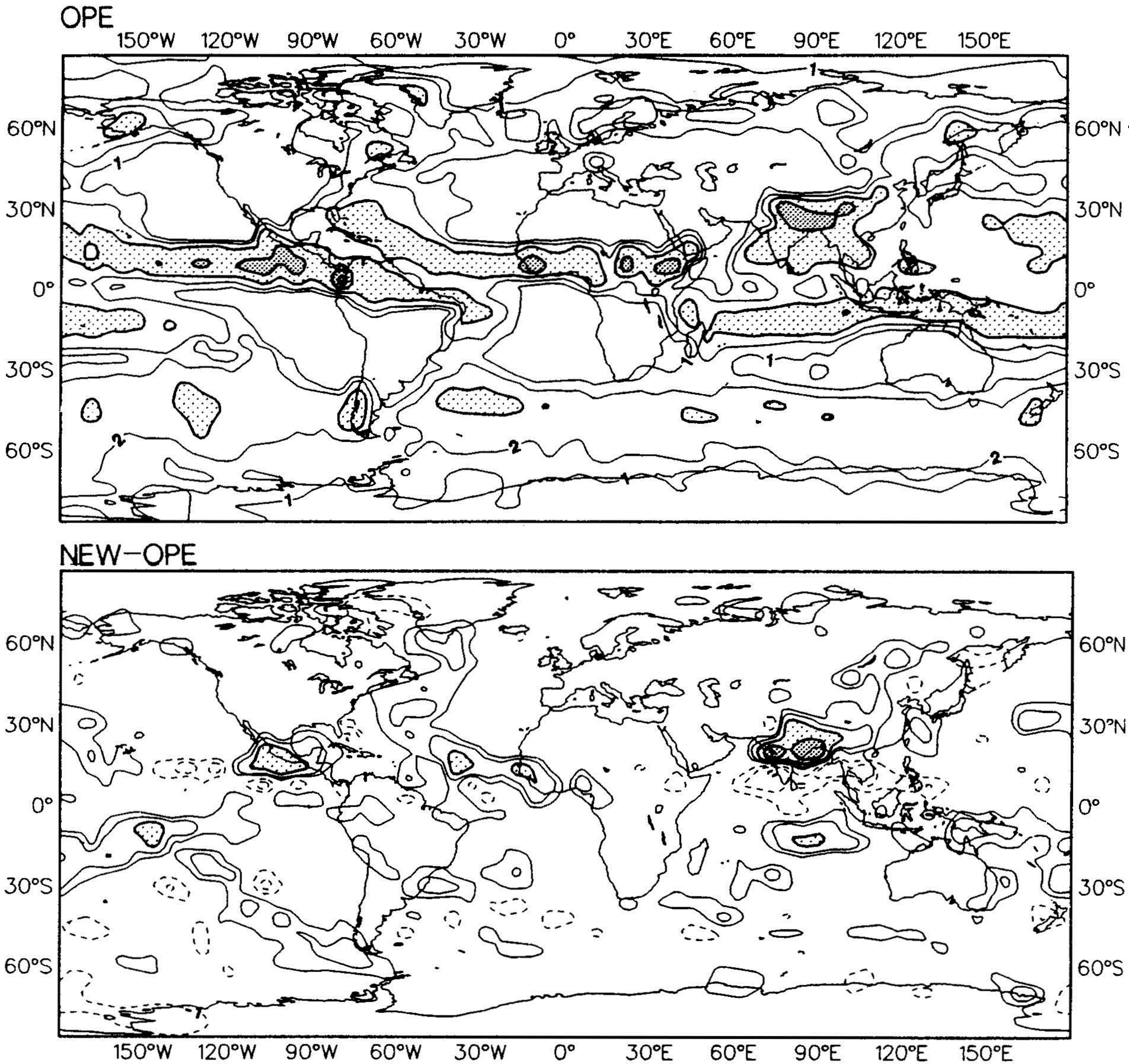

FIG. 13. Total precipitation averaged over the last 30 days of T42 90-day integrations OPE (top) and difference NEW-OPE (bottom). Initial date is 1 June 1987 (12Z). Isolines are for 1, 2, 4, 8, 16 mm day^{-1}. Values above 4 mm day^{-1} are stippled.

Increased precipitation most of it of convective.

Compatible with more surface SW radiation stronger convection, and more radiative cooling increasing the upper-level RH.

A feedback loop with hydrology and dynamics involving cloud and radiation interactions:

Riehl & Malkus (1957), Betts & Ridgway (1988)
Slingo & Slingo (1988), Randall et al. (1989)

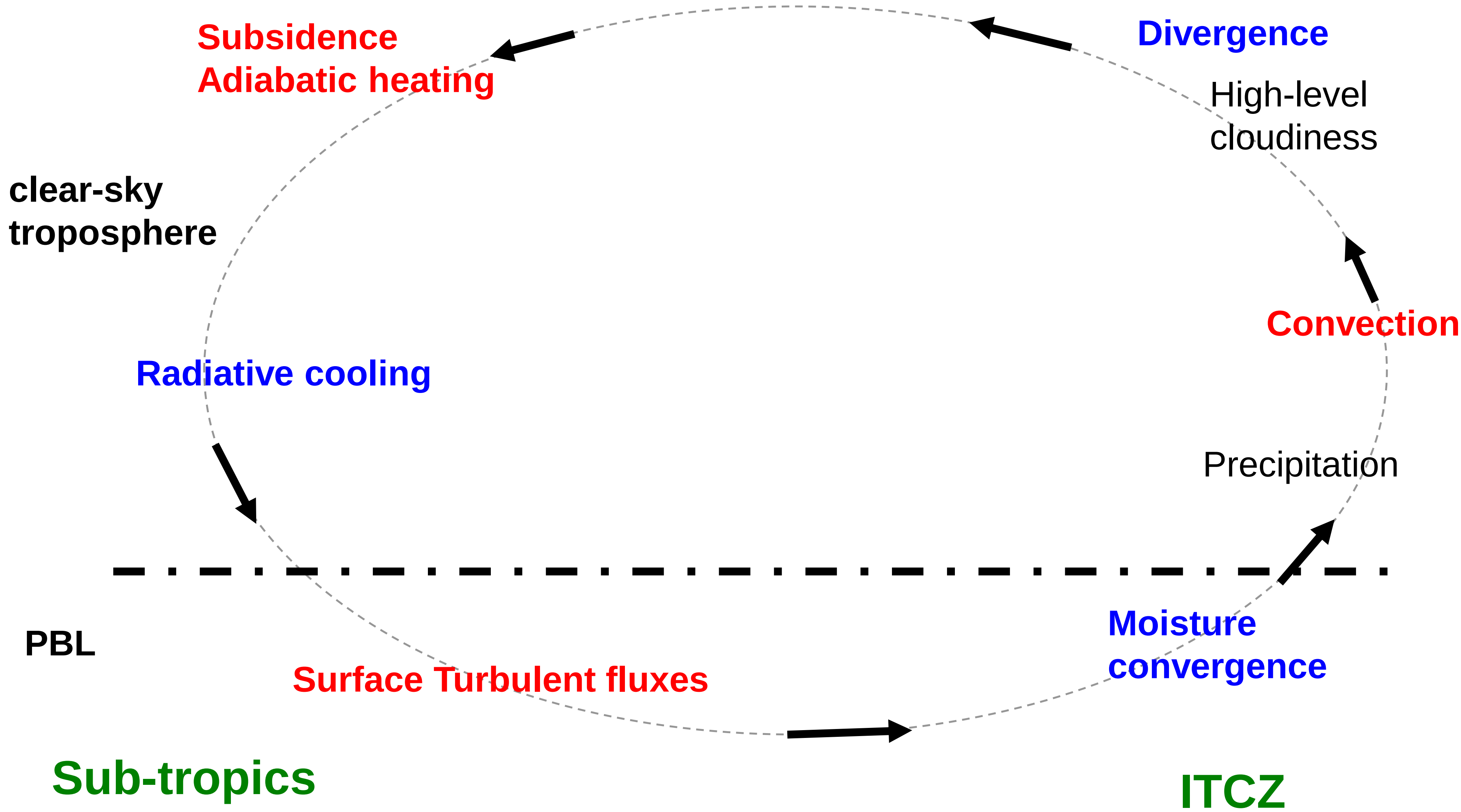

Impact on temperature

Increase in tropospheric T error with troposphere cooler by 1-1.5K, but similar latitudinal gradient

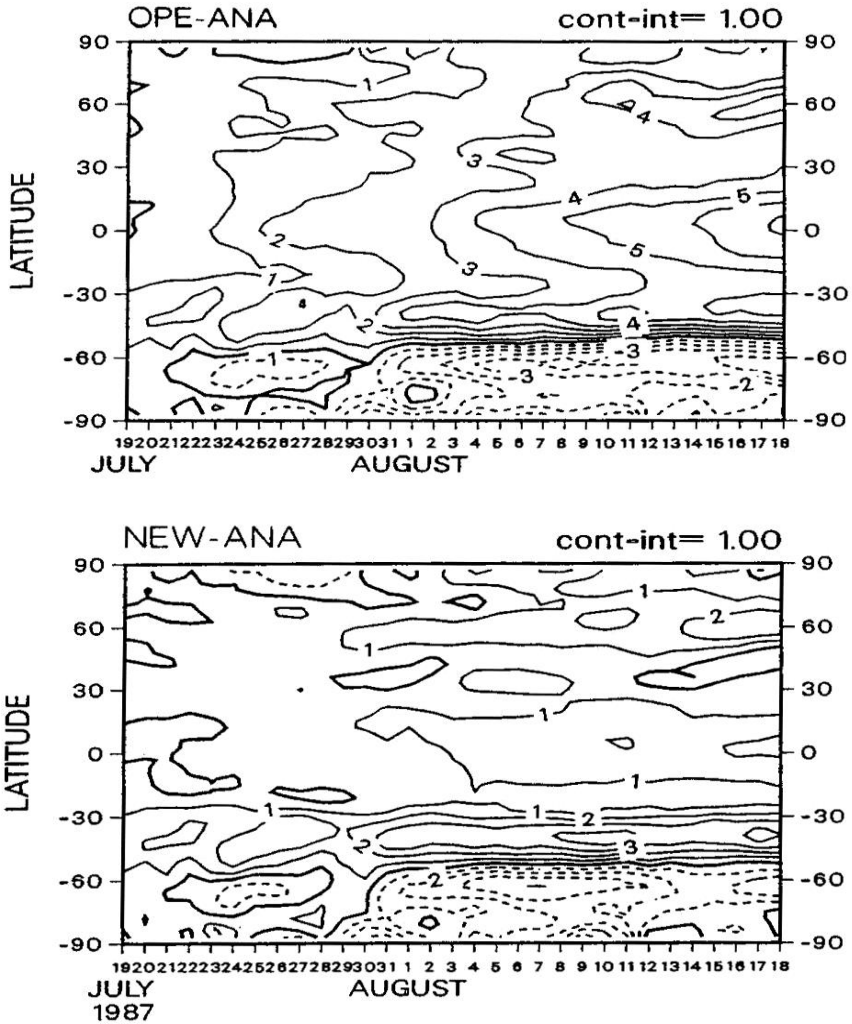

FIG. 14. Error growth of the zonal mean vertically integrated temperature above 100 hPa for T63 30-day integrations starting at 19 July 1987 (12Z) with OPE (top) and NEW (bottom). All quantities in degrees.

Slower growth of T error

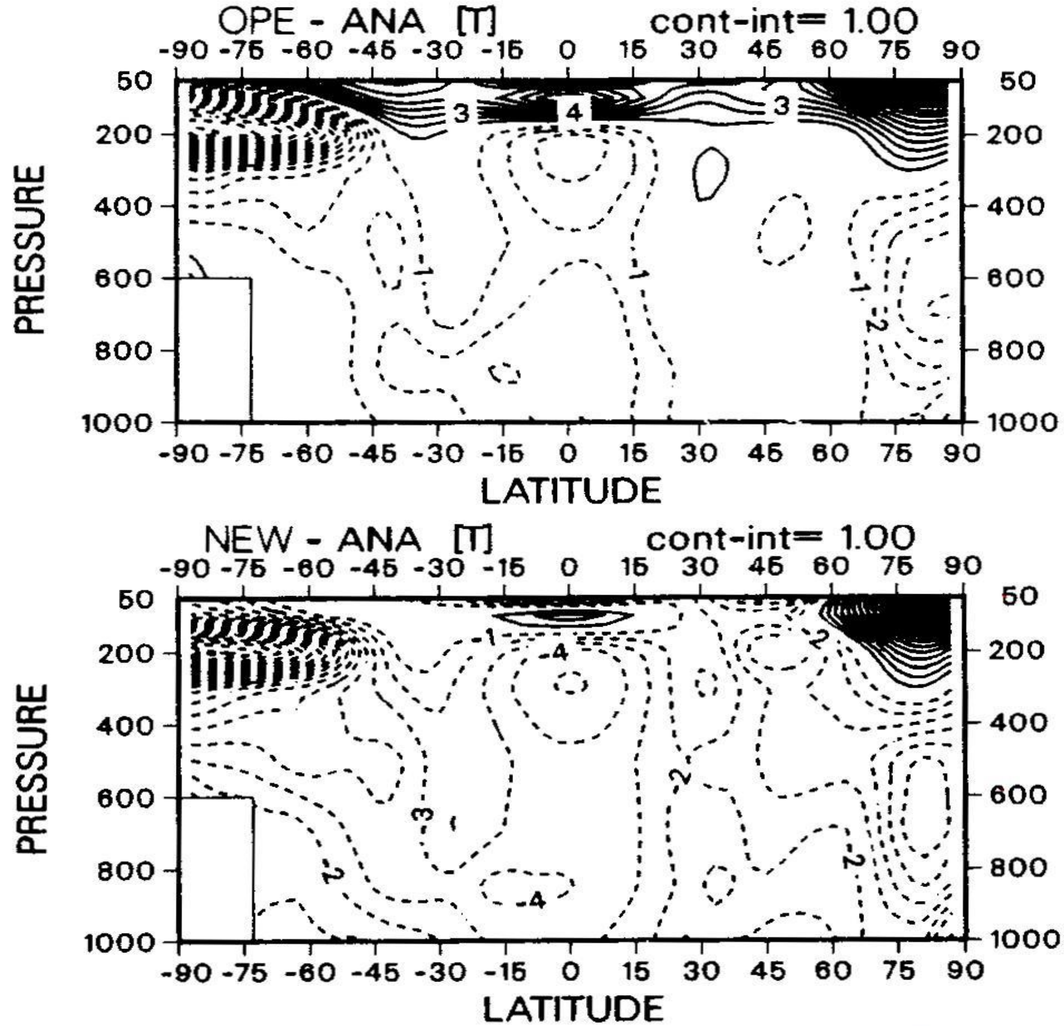

FIG. 15. Zonal mean temperature errors for day 61–90 for T42 winter simulations with OPE (top) and NEW (bottom). Initial date is 1 December 1987 (12Z).

Impact on wind

Small decrease in error (wrt analysis) for U as T latitudinal gradient remains similar. Decrease in error for W thanks to stronger convection.

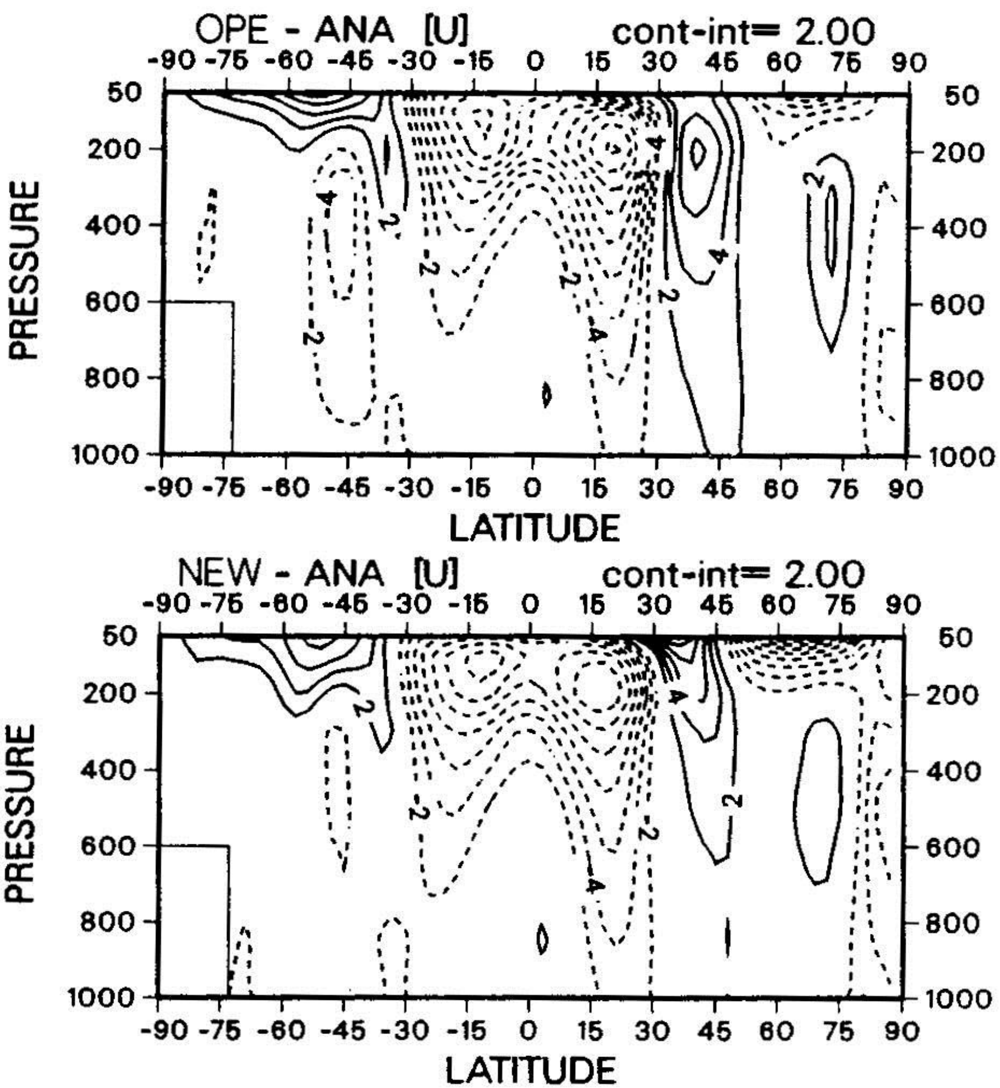

FIG. 16. As in Fig. 15, but for zonal wind (m s^{-1}).

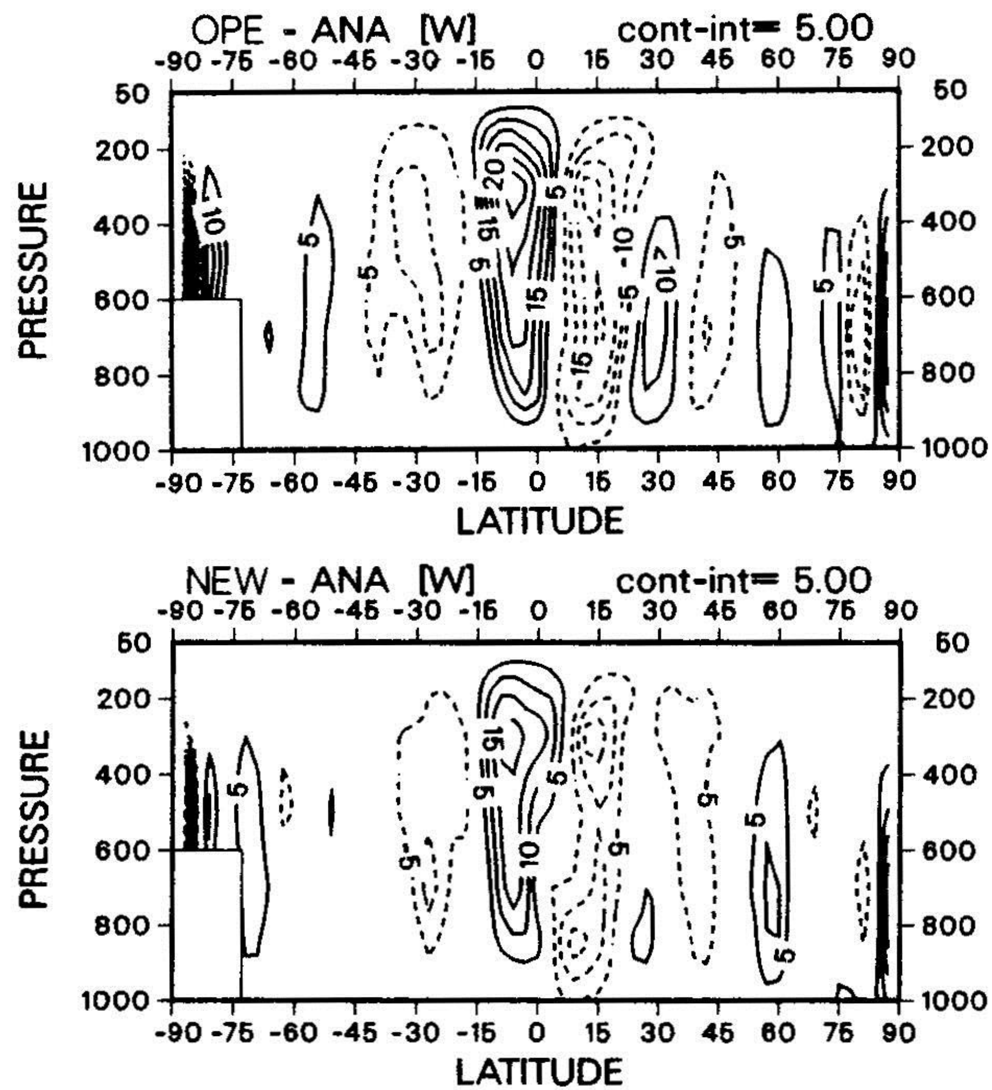

FIG. 17. As in Fig. 15, but for vertical velocity (10^{-3} Pa s^{-1}).

ECMWF

Objective scores

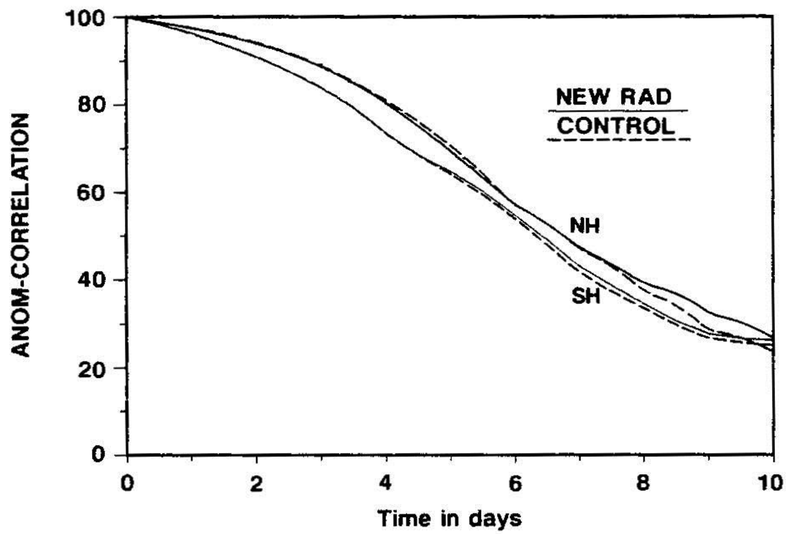

FIG. 20. Mean anomaly correlation of 1000–200 hPa heights in extratropical Northern and Southern hemispheres for 19 T63 10-day forecasts with NEW (full line) and OPE (dashed line).

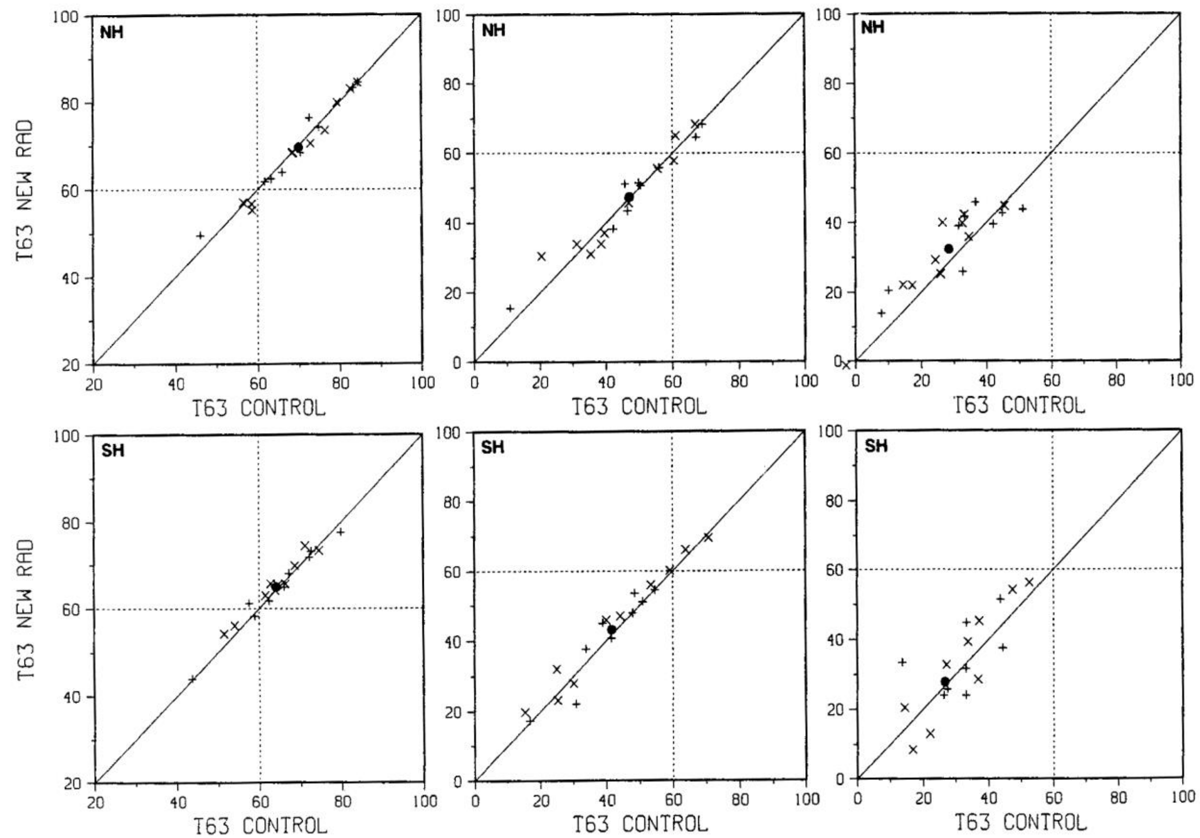

FIG. 21. Scatter of the anomaly correlation of 1000–200 hPa heights in extratropical Northern and Southern hemispheres at days 5, 7, and 9 for an ensemble of 19 T63 10-day forecasts. Improvement appears as a point above the line of slope 1.

Small impact on scores in the extra-tropics. Improvement only shows up after day 6.

Thanks to the overall improved climate behaviour of the model, the “new” radiation package became operational in May 1989.